MONTE CARLO SIMULATION OF A PROTON THERAPY BEAM LINE FOR HEAD & NECK TUMOR TREATMENT

A.Stankovskiy[1], S.Kerhoas-Cavata[1], R.Ferrand[2], C.Nauraye[2]

[1] *CEA/DSM/DAPNIA/SPhN, 91191 Gif-sur-Yvette, France,*
[2]*Institut Curie – Centre de protonthérapie d'Orsay Bât. 101 du Centre Universitaire d'Orsay, BP65-91402 Orsay, France,*
Email : Alexey.Stankovskiy@cea.fr

The Proton Therapy Center in Orsay (CPO) and CEA/DAPNIA launched the joint project on Monte Carlo modelling of a CPO beam line with the aim to achieve a prediction of dose distribution in all the calibration configurations (depth and the shape of the tumour) better than 2 %. The calculation module is intended to be used for the absolute dosimetry of the clinical beam, and in a second stage for predicting the dose distribution on a voxelized phantom constructed from the Computer Tomography (CT) patient's data. The MCNPX code was used as a basic Monte Carlo simulation tool in this study. All the elements of a CPO beam line were modelled as precisely as possible. The modelling of depth dose distribution has been improved by means of creation and implementation of the two new evaluated proton-induced nuclear data files up to 200 MeV for ^{1}H and ^{16}O. The new algorithm of multiple Coulomb scattering has been proposed to improve the dose prediction in lateral direction. The simulations of 3D dose profiles in water show very good agreement with measured data. The calculated absolute dose values in terms of Output Factors reveal rather good agreement with experimental values as well. Thus the Monte Carlo code MCNPX might be used for Quality Assurance as well as for design purposes.

I. INTRODUCTION

The use of Monte Carlo (MC) models and tools in the cancer therapy attracts growing interest worldwide. With the development of computational methods and tools and with increase of computer power, MC might substitute conventional algorithms for treatment planning and might be helpful for design purposes as well. In the proton therapy, the treatment planning tools usually are based on various parameterizations of measured proton dose distributions (so-called pencil-beam or broad-beam techniques) while the Monte Carlo simulation provides the accurate description of the almost all possible interactions of particles with matter. The disadvantage is still huge computational time making it difficult implementing in daily clinical routines.

The MCPO (Monte Carlo modelling of a CPO beam line) project launched in 2006 by the Proton Therapy Center in Orsay (CPO) and CEA/DAPNIA has the aim to achieve the accuracy of prediction the dose distribution in all the calibration configurations (depth and the shape of the tumor) better than 2 %. The MC tool is intended to be used for the absolute dosimetry of the clinical beam (patient Quality Assurance - QA), and for the calculations of dose distribution in a voxelized phantom constructed from the CT patient's data. Along with this ultimate goal, the Monte Carlo simulation tool could be helpful in better understanding of fundamental physical processes taking place in the beam delivery system while designing the beam line.

The project has 3 basic parts. First of all, the beam line has to be accurately modelled with respect to the dose delivered to water with targeted accuracy of Monte Carlo predictive power 1-2% in the absolute dose values or 1-2 mm in range necessitating to perform an extensive set of calculations and measurements of a relative dose deposited in water. This is followed by the absolute dose to water calibrations in terms of OF (Output Factors). Finally, the MC simulations will be realized in patient voxelized phantom constructed on the basis of CT data. This paper describes the first and second stages of the project.

II. METHODS

II.A. Beam line configuration

The general purpose Monte Carlo transport code MCNPX 2.5.0 [1] was chosen as the simulating tool. The brief description and basic features of MCNPX related to the proton therapy could be found in Refs. 2,3.

The CPO beam line configuration is schematically shown in Figure 1.

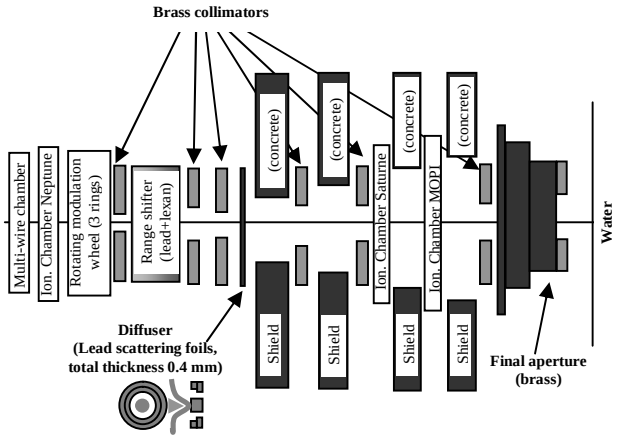

Fig.1. Composition of a beam line (not to scale). Beam is entering from the left. The distance from accelerator tube vacuum window (not shown) to water tank is about 7 m.

This line uses passive scattering technique. The raw beam (pulses of 20 μs, produced at a frequency of 448 Hz), coming from the accelerator tube, first faces the rotating wheel which modulates the proton energy spectrum. Between the accelerator tube vacuum window and the modulator, two transmission ion chambers are situated to monitor beam parameters. After being cut by the first collimator with diameter 3 cm, the beam interacts with the range shifter (so-called "binary filter") that consists of lexan and lead layers of various thicknesses. The patient-dependent range and flatness of a dose distribution are formed by the proper combination of these range shifting and pre-scattering layers. Another element of the double-scattering system, so-called "diffuser", consists of a set of thin lead foils put together as it is shown in Figure 1. Then beam enters the treatment room through a hole in the concrete shielding separating the treatment room from accelerator beam line. After passing through a number of collimators and ion chambers, the beam is finally collimated and protons deposit their energy in water. In the clinical case, the patient-dependent collimators and compensators to cover the tumor shape are attached to the final aperture.

All the elements of a CPO beam line were modelled according to the technical data provided by manufacturer. The distance between the isocenter, which for the calculations was accepted to be an entrance face of water tank, and the accelerator tube vacuum window, is about 7 m. The dose to water was scored experimentally by IBA-Scanditronix-Wellhöfer CC13 chamber with active volume of 0.13 cm^3. In MCNPX, the dose was calculated in the cylindrical volumes of the same size positioned in a chain along beam axis (for depth profiles) and perpendicular to it (for lateral profiles).

The raw beam spatial distributions measured experimentally in vertical and horizontal directions were taken as beam parameters for Monte Carlo simulations. The distributions at the exit of vacuum window are not symmetric and not exactly Gaussian, however, the similar measurements by monitor chambers placed after each collimator show that beam acquires Gaussian shape before reaching the water phantom.

The beam mean energy is suggested by the accelerator manufacturer to be 201 MeV with the energy spread 0.5% that corresponds to full-width-at-half-maximum 1.005 MeV. These values have been used as beam input parameters for Monte Carlo simulations.

The beam angular spread was measured experimentally and was found to be the Gaussian with FWHM $\Delta\theta$=4.4 mrad which has also been used as input parameter for MCNPX calculations.

II.B. Modulated beam

The simulation of modulated beam, in general, represents certain difficulties when using MCNPX since the code does not treat time-dependent geometry changes. However for modeling of a CPO beam line geometry set-up it was easily avoided. The idea behind that was to create phase space files immediately after modulator. The aluminium modulator wheel consists of three "rings" with sectors of various thicknesses. It was described within sub-millimeters in terms of MCNPX combinatorial geometry, and the routine realizing "quasi-time-dependent" simulation was created to save information on particles crossing modulator after each rotation step. This routine performs automatic transformation of the modulator geometry according to the value of rotation angle, launches the MCNPX simulation in a single processor mode (parallel calculation mode was found to be ineffective since time to send/receive subtasks from master to slave processors is comparable with typical simulation time on a single processor for each angular step) and adds particle track information to surface-source write (SSW) file. The angular rotation step was determined empirically. It should not necessarily be as small as possible. Due to FWHM of a beam impinging the modulator is about 30 mm, it is quite safe to have the next position of the wheel if the beam is centered at the half of the beam projection radius (15mm/2=7.5 mm from the previous position). Taking into account the distance from the center of modulator wheel, the angle is about 2.5° for the case of small modulation and up to 5° for the case of large modulation. Thus to have smooth particle distributions (for each particle type the energy, position, direction and momentum were scored) the 2 degree angular step of rotation was chosen with the number of primary proton tracks simulated per angular step equal to 100,000. Three surface-source read (SSR) files containing phase space for each modulation ring were created.

The use of these three distributions as new particle sources allowed to reduce significantly the computation

time. Moreover, the actual number of particle tracks (limited by the available disk storage capacity, at present about 9 millions tracks are stored in each file) might be increased in subsequent simulation to ensure the better quality of results. Each starting particle track is repeated with new random number seed. The recycling factor is ranged from 2 (for unmodulated depth profiles) to several hundreds (for lateral profiles).

Typical computing time to obtain flat depth dose profile i.e. spread-out Bragg peak (SOBP) of the quality better than 2% for dose and 1 mm for range and modulation width is about 15 min to simulate 10^7 particle histories originated from the phase space behind modulator. The cluster of nine 2 GHz processors running under Linux was used to perform calculations for this study. This seems to be acceptable from the viewpoint of further integration of Monte Carlo dose calculation into the treatment planning.

III. RESULTS AND DISCUSSION

III.A. Depth dose profiles

The secondary particles originated from nuclear non-elastic interactions of protons with materials along the beam line contribute insignificantly to the total dose delivered to water.[4] The exception is secondary protons whose contribution might be as high as 10-15% to the energy deposited proximal to single Bragg peak and in the case of SOBP, they in addition influence the flatness and may undergo another nuclear interactions. Other particles generated in nuclear interactions (deuterons, tritons, ^{3}He and alphas) are contributing less than 2%. Neutrons, electrons and photons deposit their energy far outside the irradiated volume while their contribution to dose to water is approximately 0.1%. Table 1 illustrates the contribution of each particle to the total dose delivered to water for small and large modulation.

TABLE I. Contribution of each particle type into the overall dose to water

	Contribution (%)	
Particle type	Small (SOBP with ~ 5 cm)	Large (SOBP width ~ 10 cm)
Protons (primary and secondary)	98.5	98.549
Neutrons	0.025	0.023
Photons	0.045	0.042
Electrons	0.04	0.038
Deuterons	0.83	0.8
Alphas	0.56	0.548
Total	100	100

For the purposes of 3D relative dosimetry neutrons, photons and electrons were removed from the list of transported particles that along with application of variance reduction technique accelerates the calculation of dose profiles up to a factor of 15. However, such problems as study of dose delivered by neutrons (or photons and electrons) outside the irradiated volume, as well as estimation of output factors for beam calibration, obviously require tracking all particles.

In general, of great importance is to carefully account for nuclear interactions (both elastic and non-elastic) which take place close to and inside in the irradiated volume, i.e. water tank in our case. MCNPX has two options how to treat nuclear interactions: to invoke various physics models (up to 8 combinations of intranuclear cascade, preequilibrium and evaporation models) or to sample them according to nuclear data tables read in from corresponding files. In case the data table for particular isotope is absent or the energy range of data does not span the energies characteristic to the problem, the code uses model calculations. Strictly speaking, especially for the energies characteristic to proton therapy (up to ~ 200 – 250 MeV) the data files provide more precise description of nuclear interactions than models integrated in MCNPX for two reasons: the proton induced data are evaluated from the external model calculations and experimental data, and, secondly, the quality of preequilibrium and evaporation models in MCNPX which dominate at these energies remains questionable.

The dose profiles shown in Fig.2 were calculated with proton-induced cross section data (solid curve) and MCNPX physics models for nuclear interactions (dash-dotted curve). Additional tests proved the fact that contribution of nuclear interactions occurred outside the water tank into the total dose is vanishingly small, thus the difference between two curves is mostly due to that in proton-induced cross sections for ^{1}H and ^{16}O (which almost compose the water) read in from data files and modelled inside MCNPX.

However, the proton data files available in worldwide evaluated nuclear data libraries, in general, have upper energy limit of 150 MeV which is not enough to fully cover the problem. This necessitated creation and implementation of two new evaluated data files for p+^{1}H and p+^{16}O up to 200 MeV. The evaluation methods and procedures are comprehensively described in Ref.5.

The thorough analysis for various range shifting and modulation configurations with the help of coincidence criteria manifests that the use of new evaluated data files gives more precise depth dose distributions.[5]

In the same time, due to the large underestimation of proton elastic scattering cross section on hydrogen below 150 MeV, the MCNPX model option significantly underestimates the shape of the curve (dotted curve in Figure 2). In case of SOBP the difference between model

calculations and calculations with the use of evaluated data files is more pronounced, than in case of single non-modulated Bragg curve, due to accumulation of this discrepancy when summing up the doses deposited by protons at each angular position of modulator wheel.

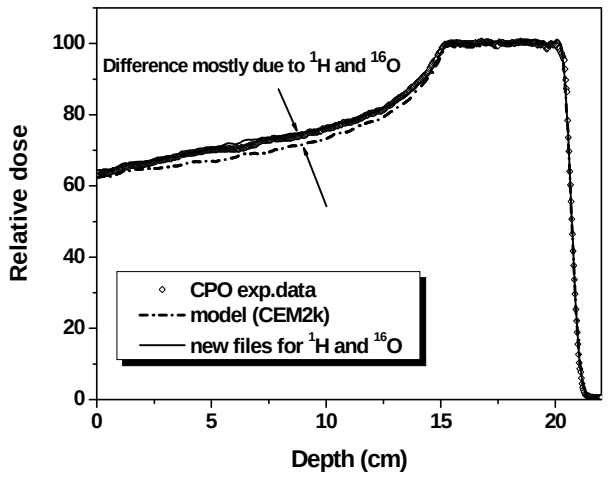

Fig.2. Depth dose distribution for modulated beam calculated with model option and new data files versus experimental data.

There was found no dependence of SOBP distal fall-off edge and lateral dose profiles from the model/data choice. The SOBP was simulated with accuracy below the experimental uncertainties, i.e. within prescribed value of 1 mm.

III.B. Lateral dose profiles

Following the discussion on MCNPX predictive capabilities as applied to proton therapy,[2] it was reported in Ref.6 that MCNPX overestimates the angular deflections, especially for high-Z materials, when protons traverse thin foils. This was found to occur due to simplified multiple Coulomb scattering (MCS) of heavy charged particles algorithm incorporated into the code.

To find how adequately the physics inside MCNPX reproduce the real dose distributions, all the beam-scattering devices, i.e. diffuser, binary filter and modulator, were removed from the line so that the beam line was composed from collimators and ion chambers only. The analysis of measured and simulated lateral dose profiles taken at the entrance of water tank revealed that the multi-wire ion chamber for beam monitoring located close to beam entry point for simulations (Figure 1), which represents 38 μm-thick stainless steel box containing tungsten wires and gas, was the key element influencing the lateral profile shape. The overestimation of scattering angle was found not only for high-Z materials, but even for stainless steel. However, the reduction of multi-wire chamber wall thickness from 38 to 15 μm allowed to obtain better agreement with measured data not only for this particular case, as it is shown in Fig.3, but for all other clinical configurations, i.e. with modulator wheel, diffuser and range shifter on the beam line.

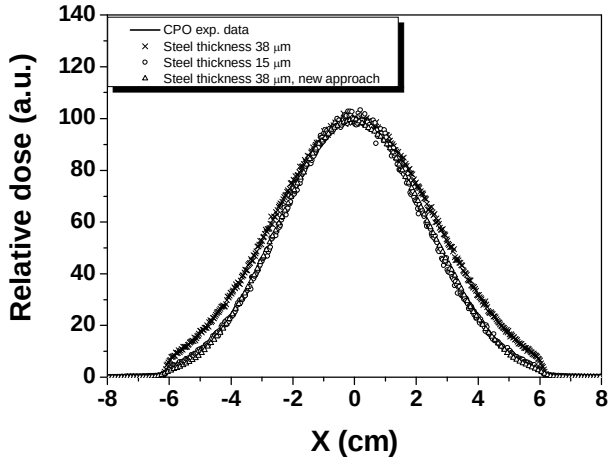

Fig.3. "Native" lateral dose profile modelled with standard MCS algorithm for different thickness of steel box, and with new MCS algorithm.

The conclusion in Ref.6 was that the MCS realization in MCNPX obviously needs improvement. However, recent investigations described below only partially confirm this statement.

III.B.1. Present MCNPX algorithm for modelling multiple Coulomb scattering of charged particles

The MCNPX algorithm of sampling the scattering angle θ, as described in Ref.7, follows the Rossi theory.[8] Following these papers describing and adopting Molière theory,[9] at the small scattering angles the angular distribution is pretty Gaussian with the characteristic scattering angle defined as follows:

$$\theta_0 = \frac{15MeV}{\beta cp} z_p \sqrt{\frac{\rho\Delta}{X_0}} \qquad (1)$$

where p, βc and z_p are the momentum, velocity and charge number of the incident particle, ρ is the mass density of the material (g/cm^3), Δ - the current tracking step length of particle in the material, X_0 – radiation length of material. Last quantity is calculated from the following equation:

$$\frac{1}{X_0} = \frac{4\alpha r_e^2 \gamma \cdot 10^{24}}{\rho} \sum_i f_i Z_i (Z_i + 1) \ln \frac{(r_e/r_0)^{1/2}}{\alpha A_i^{1/6} Z_i^{1/6}} \qquad (2)$$

Here α stands for fine structure constant, $r_e = e^2/m_e c^2$ is the classical electron radius, γ - atom density of material (barn·cm^{-1}), f_i - fraction of isotope i in material (normalized to unity), Z_i and A_i – charge and mass number of isotope i and r_0 is the nuclear radius parameter which according to Rossi is equal to $0.49 r_e$.

Then the scattering angle θ is sampled to match the Gaussian distribution:

$$\theta = \sqrt{2}\theta_0 \sqrt{\ln \frac{1}{\xi}} \qquad (3)$$

where ξ is a uniformly generated random number.

This very fast algorithm provides rather crude approximation of the scattering angle and overestimates it up to 15%, depending on the material.[10] It could not pose significant problems when dealing with the thick targets. However when the targets become thinner, the usage of this formula leads to wrong results. As it might be seen from Fig.3 (dashed line), the simulation with MCS algorithm currently incorporated in MCNPX results in about 15% over prediction of lateral penumbra. The reduction of foil thickness in the input geometry leading to correct description of relative dose profiles might not be the proper one when simulating absolute dosimetry due to the artificial change of particle fluence. This necessitated the implementation of a new algorithm for multiple scattering angle calculation in MCNPX.

III.B.2. New approach to modelling multiple Coulomb scattering of heavy charged particles

To minimize the modification of MCNPX charged particle tracking algorithm, the Molière theory has been chosen as a basis. A lot of studies have proved the validity of this theory for multiple scattering on small angles. However this theory does not provide the lateral displacement of a particle position after a given step (see Fig.4) but angular distribution only.

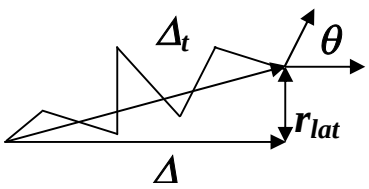

Fig.4. Multiple scattering angle θ, geometrical step length Δ, true path Δ_t and lateral displacement r_{lat} of particle after multiple scattering process.

The possibility of using the Lewis theory[11] which gives both the angular and lateral displacement distributions, as it is realized in GEANT4,[12] has been also examined. It necessitated the serious modification of a particle tracking algorithm but did not lead to better description of results that the solution described below.

The relatively fast algorithm of sampling a multiple scattering angle was proposed by Kuhn and Dodge.[13] It is based on replacement of Molière's analytical solution by Gaussian distribution with Rutherford-like tail with the requirement of the probability distribution function magnitude at $\theta = 0$ to coincide with analytical value. The probability $dP(\theta)$ of scattering into a polar angle between θ and $d\theta$ is given by

$$dP(\theta) = \left(1 - \frac{0.827}{B}\right) \exp\left[\left(-\frac{\theta}{\theta_0}\right)^2\right] \frac{d\theta}{\theta_0^2} + \Theta\left(\theta - \sqrt{2}\theta_0\right) \frac{\chi_c^2}{4} d\left(-\frac{1}{\sin^2(\theta/2)}\right) \qquad (4)$$

The characteristic scattering angle χ_c, reduced target thickness B and screening angle χ_a are defined according to Refs. 9,10:

$$\chi_c^2 = \frac{4\pi N_A \alpha^2 (\hbar c)^2 z_p^2}{\overline{A}} \left(\sum_i f_i Z_i (Z_i + 1)\right) \frac{\Delta_t}{(\beta c p)^2} \qquad (5)$$

$$B - \ln(B) = b = \ln\left(\frac{\chi_c^2}{1.167 \chi_a^2}\right) \qquad (6)$$

$$\chi_a^2 = \left(\frac{m_e c^2}{0.885 pc} \alpha \sum_i f_i Z_i^{1/3}\right)^2 \times \left(1.13 + 3.76\alpha^2 \frac{z_p^2}{\beta^2} \left(\sum_i f_i (Z_i + 1)\right)^2\right) \qquad (7)$$

Here $\overline{A} = \sum_i f_i W_i$ is the mean atomic weight of material, and Δ_t is true step length. The characteristic scattering angle is defined as follows:

$$\theta_0 = \chi_c \sqrt{(B - 1.25)} \qquad (8)$$

Prior to calculation of scattering angle the true, or corrected, path length is being calculated in a similar way to GEANT4 [12] with formulas derived from Refs.14,15.

The true path length is calculated according to

$$\Delta_t = -\lambda \ln\left(1-\frac{\Delta}{\lambda}\right),\ \Delta < \lambda \qquad (9)$$

when the value of Δ is small (i.e. the energy losses during the step are neglected), or

$$\Delta_t = r_0\left[1-\left(1-\frac{\Delta}{r_0}\left(1+\frac{r_0}{\lambda}\right)\right)^{\frac{\lambda}{\lambda+r_0}}\right] \qquad (10)$$

when the energy losses are taken into account. Here λ stands for the transport mean free path and r_0 is the particle range at the beginning of step.

The value of this limiting step is the model parameter and has been set to 1 μm to fit the experimental data.

Then, using the Δ_t, a multiple scattering angle is sampled according to distribution (4). The transcendental equation (6) is solved according to approximate formula [15]

$$B = \frac{b}{2}\left(1+\frac{\ln b}{b-1}\right)\left(1+\sqrt{1-\frac{1}{b}}\right)+C \qquad (11)$$

with the value of C=0.295 instead of zero in Ref.16. Then the value of B is increased by 1 to minimize discontinuity at $\theta = \sqrt{2}\theta_0$ between Gaussian part and Rutherford-like tail.[13]

The validity range of Molière theory might be derived from eq.(6) with the lower limit defined by the condition $B > 1$ (or $b \geq 1$) and upper limit being $\chi_c^2 B \leq 1$:

$$e\cdot\frac{1.167\chi_a^2(pv)^2\overline{A}}{4\pi N_A\alpha^2(\hbar c)^2 z_p^2\left(\sum_i f_i Z_i(Z_i+1)\right)} < \Delta_t < \frac{(pv)^2\overline{A}}{4\pi N_A\alpha^2(\hbar c)^2 z_p^2\left(\sum_i f_i Z_i(Z_i+1)\right)\cdot B} \qquad (12)$$

where e stands for the base of natural logarithm.

If the value of Δ_t is less than above minimum value, the standard MCNPX calculation of θ is applied, while if Δ_t exceeds upper limit the angle is sampled from Rutherford-like distribution. In case of validity of (12) the angle is sampled with random number ξ according to Gaussian part of the distribution if $\theta \leq \sqrt{2}\theta_0$:

$$\theta = \theta_0\sqrt{\ln\left(\frac{1-0.827/B}{1-0.827/B-\xi}\right)}, \qquad (13)$$

when $\xi < 1-0.827/B$.

Otherwise the Rutherford-like tail is sampled with $\xi' = P(\pi)-\xi$:

$$\theta = 2\arcsin\left(\frac{\chi_c\sin\left(\theta_0/\sqrt{2}\right)}{\sqrt{\chi_c^2-4\xi'\sin^2\left(\theta_0/\sqrt{2}\right)}}\right) \qquad (14)$$

where

$$P(\pi) = 1-0.827\Big/\left(B+\frac{\chi_c^2}{4}\left(\frac{1}{\sin^2\left(\theta_0/\sqrt{2}\right)}-1\right)\right) \qquad (15)$$

denotes the total probability of the projectile to scatter into the angle between 0 and π.

When the value of true step length falls below of some limiting step size (typically 10^{-6} mm) the single or plural scattering model might be applied instead of procedure described above with θ defined from screened Rutherford cross section.[12] However no significant contribution into scattering angle spectra was observed when comparing to calculations performed without this option, thus it might be omitted at least with the geometry setup with the foil thickness above 1 μm.

Figure 5 represents the comparison of the angular distribution of 1-MeV protons after traversing the 5 μm-thick ^{12}C target. It could be seen that standard MCNPX algorithm significantly overestimates the scattering angle while the calculation using improved algorithm gives significantly better agreement with analytical curve.

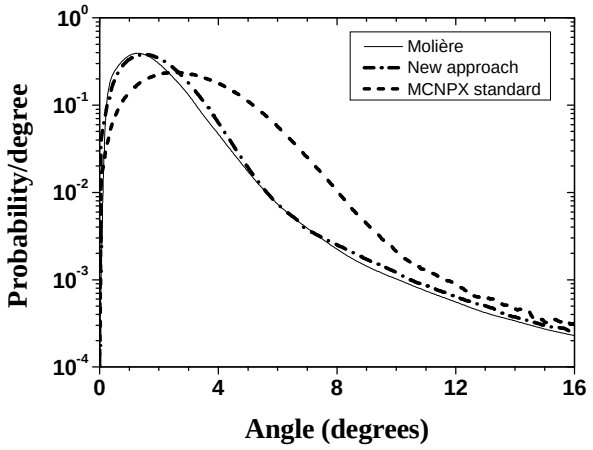

Fig. 5. Probability distribution of deflection angles for 1 MeV protons after traversing 5 μm of ^{12}C. The analytical curve produced using Molière algebra was taken from Ref.13.

As it is seen from Fig.3, where the results of "native" beam line simulations (i.e. without of three principal scattering elements – diffuser, range shifter and modulator) are plotted against experimental data, the new approach gives better agreement without any tuning of input geometry. Thus the new approach satisfactory describes the experimental data for thin foils.

Figure 6 represents the comparison of calculation results and experimental data for the clinical case when the diffuser, range shifter containing 20 mm of lexan and 2 mm of lead, and small modulator (ring 1) are installed on the beam line. In this case the relative dose distributions for both standard MCNPX algorithm and new approach for multiple Coulomb scattering of charged particles give comparable results. The multiplication of MCS processes when particles (mostly protons) traverse thick targets diminishes the disagreement between average scattering angle modelled in these two ways.

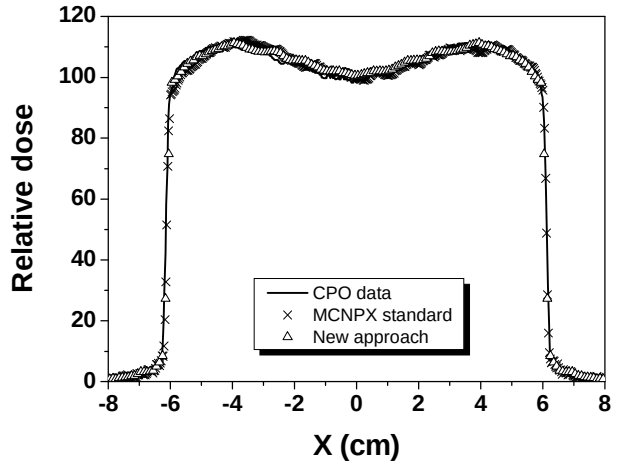

Fig.6. Relative lateral dose profiles for small modulation (ring 1) and range shifter containing 20 mm of lexan and 2 mm of lead. Solid curve represents experimental data, crosses show the calculation results with standard MCS algorithm, open triangles correspond to calculation results with new MCS approach.

The cost of the MCS improved description is about 30% in computation time. Taking into account the purpose to fast and correctly reproduce the 3D dose distribution, it might be concluded that there is no need to use improved MCS algorithm for the purpose of relative dosimetry. It might find its place when using the code for absolute dosimetry as well as for designing purposes. Also for several test cases the increase from 15 to 25% (depending on the beam line configuration) of total energy deposited in water (i.e. dose to water) was observed when using new MCS algorithm.

III.C. Output Factors

For the patient treatment, the dose calibration is performed at CPO on a regular basis to determine the proton fluence required to deliver prescribed dose to a patient. This fluence is specified in Monitor Units (MU) that corresponds to a fixed amount of charge collected in the ionization chamber 'Saturne" which is located about 2 m upstream of the isocenter (Fig.1). As it is defined elsewhere,[17,18] the output factor (OF) is determined as the ratio of the dose delivered to a calibration point divided by required MU. Due to MCNPX tallies the particle fluence rather than flux, to model OF the ratios of the dose (deposited energy) scored at two SOBP points, namely at the entrance of water tank and in the middle of the plateau, to the dose delivered to a calibration point (dose to air behind "Saturne" chamber) have been measured experimentally and calculated with MCNPX. The IBA-Scanditronix-Wellhöfer CC13 chamber with active volume 0.13 cm^3 was used for dose measurements both in air and in water. The scoring volume is enclosed between two graphite electrodes, the outer one representing the union of hemisphere and cylinder. This chamber was precisely modelled within sub-millimeters in MCNPX and the dose was scored separately in air and in water in two code runs to better reproduce experimental conditions since even this small chamber installed on the bench modifies the dose distribution in water. The scoring of OF in a single code run described in Ref.17 where the calibration point in air is located near water phantom has been found inappropriate in the case of a CPO beam line where the dose scoring points are quite far from each other (~2 m). In addition, for the purpose of absolute dosimetry it is necessary to transport neutrons, photons and electrons as well as protons, deuterons, tritons, ^{3}He, α-particles and pions. Thus the computing time becomes much greater compared to relative dosimetry. About 500 millions of particle histories have been simulated to achieve the statistical uncertainty 1%. The typical running time to obtain one pair of deposited energy values (in water and in air) is about 2 days on 9-processor cluster.

A dozen representative clinical configurations have been analyzed by now. The OF dependencies from $(R-M)/M$ values where R stands for the range of protons in water and M is the modulation width (width of SOBP plateau) are presented in Fig.7. All the calculated OF are found to be within an experimental error (2%).

There are no signs that the thorough verification on a wider range of test configurations which is currently underway will produce the deviations from experimental OF larger than presented on Fig.7.

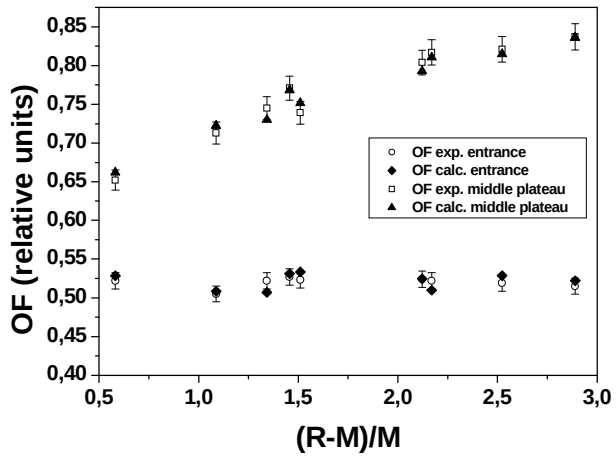

Fig.7. Measured and simulated OF as a function of $(R-M)/M$. The measured values are shown with experimental error 2%.

Consequently MCNPX reveals the capability both for relative and absolute dosimetry.

IV. CONCLUSIONS

Monte Carlo simulation for CPO treatment head geometry has been realized using MCNPX 2.5.0 code. The validation performed with reference data reveals good agreement within 1-2 mm in range, modulation width, distal and lateral penumbra for all sets of data (more than 40 depth and lateral dose distributions for modulated and unmodulated beam were simulated). The use of new evaluated proton-induced nuclear data files up to 200 MeV for ^{1}H and ^{16}O allowed to improve the predictive power of MCNPX depth dose calculations. The new algorithm of multiple Coulomb scattering of heavy charged particles gives the better agreement of calculated relative dose distributions with experimental data for thin foils, however for clinical cases the standard MCS algorithm incorporated in MCNPX remains competitive. The output factors calculated for several test configurations reveal good agreement with experimental data thus proving the MCNPX capability for absolute dosimetry as well.

ACKNOWLEDGMENTS

The authors appreciate S.Meyroneinc (CPO) for fruitful discussions and P.-F.Honore (CEA) for organizing and supporting cluster calculations.

REFERENCES

1. D. B. PELOWITZ, ed. MCNPX User's Manual, Version 2.5.0 LA-CP-05-0369 (2005).
2. J. HÉRAULT, N. IBORRA, B. SERRANO and P. CHAUVEL, "Monte Carlo Simulation of a Protontherapy Platform Devoted to Ocular Melanoma", *Med. Phys.*, **32 (4)** 910 (2005).
3. W. NEWHAUSER, N. KOCH, S. HUMMEL, M. ZIEGLER and U. TITT, 'Monte Carlo Simulations of a Nozzle for the Treatment of Ocular Tumors with High-Energy Proton Beams", *Phys. Med. Biol.*, **50,** 5229 (2005).
4. H. PAGANETTI, *Phys. Med. Biol*., **47,** 747 (2002).
5. A. STANKOVSKIY, S. KERHOAS-CAVATA, R. FERRAND and C. NAURAYE, " Monte Carlo Simulation of a CPO Beam Line: Modeling the Nuclear Interactions", *Proc. Int. Conf. on Nuclear Data for Science and Technology ND-2007*, Nice, France, 23-27 April 2007, to be published (2007).
6. A. STANKOVSKIY, S. KERHOAS-CAVATA, R. FERRAND and C. NAURAYE, "Simulation of the Patient Quality Assurance on a CPO Beam Line", *J. Phys: Conf. Ser.*, to be published (August 2007).
7. R. E. PRAEL, Multiple Coulomb Scattering Methods in LAHET3 and MCNPX, Los Alamos research note LA-UR-02-0425 (2002).
8. B. ROSSI, *High Energy Particles*, Prentice-Hall, Englewood Cliffs, NJ (1952).
9. G. MOLIÈRE, *Z.Naturforsch*., **3a**, 78 (1948).
10. B. GOTTSCHALK, "Passive Beam Spreading in Proton Radiation Therapy (draft), http://huhepl.harvard.edu/˜gottschalk (2004).
11. H.W.Lewis, "Multiple Scattering in an Infinite Medium", Phys. Rev., **78 (5)**, 526 (1950).
12. GEANT4 Physics Reference Manual, http://geant4.web.cern.ch/geant4/, p.67-80.
13. S. E. KUHN AND G. E. DODGE, A Fast Algorithm for Monte Carlo Simulations of Multiple Coulomb Scattering, *Nucl. Instr.Meth. in Phys. Res.* **A322**, 88 (1992).
14. J. M. FERNANDEZ-VAREA et al., *Nucl. Instr.Meth. in Phys. Res.* **B73,** 447 (1993).
15. I. KAWRAKOW and ALEX F. BIELAJEW, *Nucl. Instr.Meth. in Phys. Res.* **B142**, 253 (1998).
16. S. I. STRIGANOV, "On the Theory and Simulation of Multiple Coulomb Scattering of Heavy Charged Particles", *Rad. Prot. Dosimetry*, **116(1-4)**, 293 (2005).
17. H.PAGANETTI, "Mone Carlo Calculations for Absolute Dosimetry to Determine Machine Outputs for Proton Therapy Fields", *Phys. Med. Biol*., **53**, 2801 (2006).
18. J. HÉRAULT, N. IBORRA, B. SERRANO and P. CHAUVEL, "Spread-out Bragg Peak and Monitor Units Calculation with the Monte Carlo Code MCNPX ", *Med. Phys.*, **34 (2),** 680 (2007).